PupilHeart: Heart Rate Variability Monitoring via Pupillary Fluctuations on Mobile Devices

Xiangyu Shen, Hongbo Jiang, *Senior Member, IEEE*, Daibo Liu, *Member, IEEE*, Kehua Yang, Feiyang Deng, Taiyuan Zhang, Zhu Xiao, *Senior Member, IEEE*, John C. S. Lui, *Fellow, IEEE*, Jiangchuan Liu, *Fellow, IEEE*, Schahram Dustdar, *Fellow, IEEE*, and Jun Luo, *Senior Member, IEEE*

Abstract—Heart disease has now become a very common and impactful disease, which can actually be easily avoided if treatment is intervened at an early stage. Thus, daily monitoring of heart health has become increasingly important. Existing mobile heart monitoring systems are mainly based on seismocardiography (SCG) or photoplethysmography (PPG). However, these methods suffer from inconvenience and additional equipment requirements, preventing people from monitoring their hearts in any place at any time. Inspired by our observation of the correlation between pupil size and heart rate variability (HRV), we consider using the pupillary response when a user unlocks his/her phone using facial recognition to infer the user's HRV during this time, thus enabling heart monitoring. To this end, we propose a computer vision-based mobile HRV monitoring framework-PupilHeart, designed with a mobile terminal and a server side. On the mobile terminal, PupilHeart collects pupil size change information from users when unlocking their phones through the front-facing camera. Then, the raw pupil size data is preprocessed on the server side. Specifically, PupilHeart uses a 1-D convolutional neural network (1-D CNN) to identify time series features associated with HRV. In addition, PupilHeart trains a recurrent neural network (RNN) with three hidden layers to model pupil and HRV. Employing this model, PupilHeart infers users' HRV to obtain their heart condition each time they unlock their phones. We prototype PupilHeart and conduct both experiments and field studies to fully evaluate effectiveness of PupilHeart by recruiting 60 volunteers. The overall results show that PupilHeart can accurately predict the user's HRV.

Xiangyu Shen, Hongbo Jiang, Daibo Liu, Kehua Yang, Taiyuan Zhang, and Zhu Xiao are with the College of Computer Science and Electronic Engineering, Hunan University, Changsha 410082, Hunan, China (e-mail: shenxiangyu@hnu.edu.cn; hongbojiang@hnu.edu.cn; dbliu@hnu.edu.cn; khyang@hnu.edu.cn; taiyuanzhang@hnu.edu.cn; zhxiao@hnu.edu.cn).

Feiyang Deng is with the Chow Yei Ching School of Graduate Studies, City University of Hong Kong, Hong Kong (e-mail: feiyadeng2-c@my.cityu.edu.hk).

John C. S. Lui is with the Computer Science and Engineering Department, The Chinese University of Hong Kong, Hong Kong (e-mail: cslui@cse.cuhk.edu.hk).

Jiangchuan Liu is with the School of Computing Science, Simon Fraser University, Burnaby, BC V5A 1S6, Canada (e-mail: jcliu@sfu.ca).

Schahram Dustdar is with the Department of Computer Science, TU Wien, 1040 Vienna, Austria (e-mail: dustdar@infosys.tuwien.ac.at).

Jun Luo is with the School of Computer Engineering, Nanyang Technological University, Singapore 639798 (e-mail: junluo@ntu.edu.sg).

Digital Object Identifier 10.1109/JIOT.2023.3277555

Index Terms—1-D convolutional neural network (1-D CNN), heart monitoring, pupil-heart model, pupillary response, recurrent neural network (RNN).

I. INTRODUCTION

HEART is the most important organ of the human body, pumping blood to tissues and organs throughout the body and maintaining normal metabolism [1]. Heart disease can bring significant impacts on the safety of human life. According to the World Health Organization (WHO), about 17.5 million people die of heart disease each year, accounting for 30% of mortality [2]. Therefore, monitoring heart health in one's everyday life is of great importance to human beings.

A typical indicator used to evaluate heart health is heart rate variability (HRV) [3], [4], also known as heart rate volatility, which is simply a measure of the variation in time between each heartbeat [5]. On the other hand, it also contains the implicit information on the regulation of cardiovascular system by neuro-humoral factors, and thus can be used to diagnose or prevent cardiovascular and other diseases. Moreover, according to [6], measurements of HRV and the quantification of its spectral components are powerful predictors of cardiovascular morbidity and mortality. Therefore, it may help assess the return to work of patients with ischemic heart disease. Clinical analysis of HRV can reflect activity and balance of the cardiac autonomic nervous system (ANS) and related pathological states, etc. [7]. In general, low HRV is considered a sign of current or future health problems because it shows your body is less resilient and struggles to handle changing situations. It is also more common in people who have higher resting heart rates. That is because when your heart is beating faster, there is less time between beats, reducing the opportunity for variability. This is often the case with conditions like diabetes, high blood pressure, heart arrhythmia, asthma, anxiety and depression. In other words, heart health monitoring can be achieved by monitoring HRV.

Currently, there are two main categories of heart rate monitoring systems: 1) medical and 2) consumer heart rate monitors [8]. Medical heart rate monitors used in hospitals are usually wired and use multiple sensors, such as commonly used electrocardiogram machines in hospitals [9]. Meanwhile, portable medical devices also have been developed, which are called Holter monitors [10]. On the other hand, consumer heart rate monitors are designed for everyday use and are wireless.

Specifically, there are two types of consumer heart rate monitors: electrical-based and optical-based [11]. The electrical monitors consist of two parts: 1) a monitor/transmitter worn on a chest strap and 2) a receiver. When a heartbeat is detected, a radio signal is transmitted, which is used by the receiver to display/determine the current heart rate [4], [12]. Instead, the optical-based heart monitoring system measure the heart rate by shining light from an LED light across the skin and evaluating how it scatters off blood vessels, such as the popular smart watches [13], [14]. However, all these existing methods either require professional guidance or additional equipment, which is inconvenient for daily heart rate monitoring and increases cost of devices.

In this context, we raise a question: *can we monitor users' HRVs through some daily activities and without additional equipment and professional guidance?* Recent studies have shown that both pupils and heartbeat are controlled by same nerves, i.e., sympathetic and parasympathetic nerves [15], [16]. Thus, changes in the pupil are correlated with variations in the heartbeat. For example, when a person is frightened, the sympathetic nerve strengthens while the parasympathetic nerve weakens, resulting in a faster heartbeat and a smaller pupil diameter. Based on this principle, we explore the quantitative correlation between pupil size and HRV. In addition, with the development of modern technology, the smartphone ownership is growing, and the number of smartphones based on facial recognition unlocking is also increasing. According to [17], [18], more than 800 million users around the world have smartphones with the function of face recognition and users unlock their phones 50 times on average per day. Therefore, we consider using the front-facing camera of mobile phones to record the change of user's pupils while he/she unlocks the phone with facial recognition while obeying the privacy policy, so as to achieve HRV monitoring of the user. If it works, pupil-based mobile HRV monitoring can bring some unique advantages over existing methods.

1) *Convenience:* Monitoring HRV on mobile devices is much more portable than professional equipment and does not require special instruments or professional guidance.

2) *Accuracy:* HRV monitoring based on mobile device unlocking involves different time periods and different physiological and mental states of users, which provides more samples and thus guarantees the accuracy of HRV monitoring.

In our study, we first investigate the initial qualitative relationship between the heartbeat and the pupil size captured by the front camera of mobile phones. Based on this, we do a further job of infering HRV from pupillary response more comprehensively and accurately. Achieving this goal entails several key technical challenges. First, the physiological process of pupillary response is intricate: it is possible to extract some features from this process, but it is difficult to identify features that are relevant to HRV. Moreover, having found the features of pupillary response, it is hard to correspond directly to HRV. Last but not least, in mobile scenarios, certain specific challenges are posed. For example, changes in light intensity or shaking may have a serious impact on the recorded face images.

Aiming to address these challenges, we hereby propose PupilHeart as the first mobile HRV monitoring system exploiting pupillary response (i.e., change of pupil size in time domain). As shown in the figure, PupilHeart exploits the heart-eye relationship in the ANS to infer HRV from pupil size changes for heart health monitoring. First, we conduct extensive studies to show the general relationship between HRV and pupil size for people in different states. This enables us to identify high-dimensional time-series features associated with HRV by using a 1-D convolutional neural network (1-D CNN). In addition, to handle the diversity of pupillary responses and HRVs in different situations, we employ a recurrent convolutional network [recurrent neural network (RNN)]-based approach to automatically train pupil-HRV model, correlating with users' pupillary responses.

We have prototyped PupilHeart on mobile phones and conducted extensive experiments to evaluate its performance in predicting HRV. Experimental results show that PupilHeart is able to accurately predict users' HRV with an average precision of 91.37%. In summary, our main contributions are summarized as follows.

1) We conduct an in-depth study of the relationship between HRV and pupil size in mobile scenarios. To the best of our knowledge, this is the first work to explore the quantitative relationship between people's pupillary response and HRV on mobile devices.

2) High-dimensional time-series features associated with user's HRV are identified by using a 1-D CNN to excavate the general physiological processes of pupillary responses.

3) We use RNN to train the high-dimensional time-series features extracted by 1-D CNN so as to model the relationship between pupil and HRV.

4) We validate the effectiveness of PupilHeart through an extensive trial by recruiting a total of 60 volunteers.[1] The results show that the accuracy of PupilHeart achieves up to 91.37% on average.

The remainder of this article is organized as follows. In the next section, we first review the related works of PupilHeart. Then, we explore the relationship between pupil diameter and user heart rate in Section III. We describe the technical details of PupilHeart in Section IV. The performance evaluations of PupilHeart is presented in Section V. Limitations of this work are discussed in Section VI, and finally we conclude this work in Section VII.

II. RELATED WORK

In this section, we review the efforts of researchers in mobile HRV monitoring and provide a comprehensive overview of the PupilHeart's advantages compared to state-of-the-art works.

A. Diverse Mobile HRV Monitoring

In recent years, researchers have paid more attention to monitor people's HRV in mobile scenarios. We roughly categorize those methods into two groups.

---

[1]Our study was approved by our university IRB. It did not raise any ethical issues.

Methods in the first group exploit photoplethysmography (PPG) to measure HRV [19], [20], [21], [22], [23], [24], [25]. Specifically, the mechanism mentioned in [19] works by placing a finger on the phone camera while turning on its flash and calculating the amount of light absorbed by the finger tissues by taking photos from the phone camera to calculate heart rate. Moreover, Bolkhovsky et al. [20] used both Android phones and iPhones to capture RR intervals and then derive HRV through a complex algorithm. In addition, the effect of sampling rate between Android phones and iPhone on the accuracy of HRV measurements is also explored. Mobile phone PPG is also advocated by Plews et al. [21], showing that PPG correlated almost perfectly with ECG, with acceptable technical error in estimation and minimal differences in standard deviations. The rolling shutter camera mechanism has been utilized to extract CIS-photoplethysmography (CPPG) data points from CMOS image sensor (CIS) pixel rows, enabling the extraction of high frame rate CPPG signals from a common built-in low frame rate smartphone's CIS [25]. As for the specific applications, PPG is utilized as a tool to estimate HRV in patients with spinal cord injury (SCI) [24].

As to the methods of the second group, they measure HRV by seismocardiography (SCG), a simple and noninvasive method of recording cardiac activity from the body movements caused by heart pumping. In a preliminary study, Ramos-Castro et al. [26] used a smartphone to record this movement and estimate heart rate. Wang et al. [27] used chest vibrations due to heartbeat as a biometric feature to authenticate users on mobile devices. Moreover, Scarpetta et al. [28] described a method based on simultaneous measurement of heartbeat and respiratory intervals with a smartphone. Specifically, a commodity accelerometer of the smartphone is used to measure SCG signal generated by heart activity and the acceleration generated by respiratory movements. In addition, Urzeniczok et al. [29] presented a mobile application for measuring heart rate in real time based on SCG, where the heartbeat is detected using a modified version of the Pan–Tompkins algorithm.

All of the above methods measure HRV based on PPG or SCG. In this work, we used a different strategy to measure HRV based on features of pupillary response, breaking the limitation that measurement from PPG and SCG requires the user to be in a steady state all the time or with help of additional equipment. To our knowledge, this is the first work to monitor user's HRV by pupil information on mobile devices.

B. Connecting Pupil With HRV

In previous investigations of the pupillary response, many researchers have probed the relevance of this physiological response to the user's heart rate variability. Schumann et al. [30] explored how sympathetic activity can lead to pupillary instability. Hung and Zhang [31] mentioned the presence of heart rate variability (HRV) and blood pressure variability (BPV) in pupil size variability (PSV). Wang et al. [15] described how pupil size is modulated by autonomic arousal. Urrestilla and St-Onge [32] suggested that cognitive load can be achieved through HRV measurements,
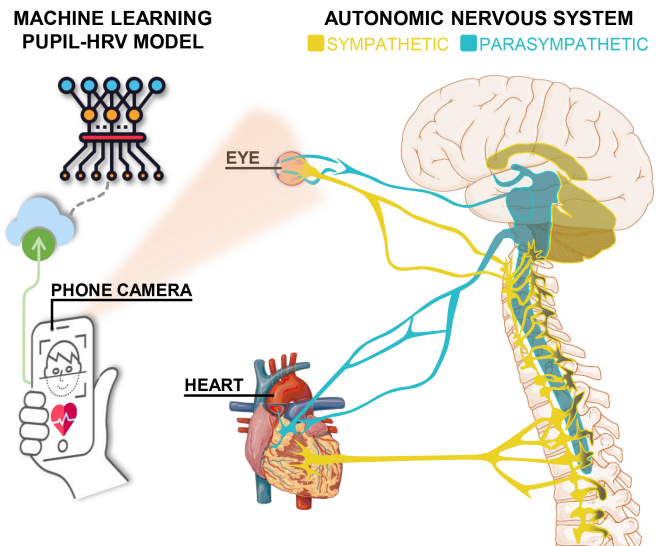

Fig. 1. PupilHeart: A novel heart monitoring system observing your eyes, rather than your heart.

brainwave monitoring, pupil measurements and even skin conductivity. Daluwatte et al. [33] studied two ANS measures in healthy 8–16 year old children aged 8–16 years for potential interrelationships between two ANS measurements: 1) pupillary light reflex (PLR) and 2) heart rate variability (HRV). None of the recommendations mentioned above take into account external factors. However, different kinds of disturbances may exist in real scenarios, such as illumination conditions and sudden changes in the person's motion state.

In this article, we consider the relationship between pupillary response and user's HRV from a distinct perspective. Specifically, we explore how changes in pupil diameter reflect the user's HRV under mobile conditions, hence supplementing and promoting nowadays mobile HRV monitoring systems.

III. MOTIVATION

In this section, we start by exploring the relationship between pupillary response and HRV from neurosciences aspects, and then conduct extensive studies to qualitatively analyze the relations.

According to existing researches [34], [35], as shown in Fig. 1,[2] pupil and heart are controlled by same nerves, namely, sympathetic nervous system (SNS) and parasympathetic nervous system (PNS). Furthermore, [15] shows that pupil size on a trial-by-trial basis particularly before face presentation correlated with both heart rate and galvanic skin response, respectively, indexing activity of parasympathetic and sympathetic branches of the ANS. For example, when people are frightened, their SNS is activated and PNS is suppressed, causing physiological changes, such as dilated pupils and rapid heartbeat.

Specifically, we utilize relative pupil size as a metric of pupillary response. Relative pupil size denotes the pupil to iris ratio. The reason is that human eye is at full size by the time

[2]The Figure was partly generated using Servier Medical Art, provided by Servier, licensed under a Creative Commons Attribution 3.0 unported license.
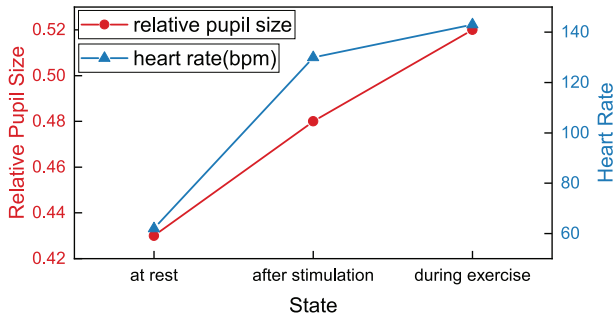
Fig. 2. Average relative pupil size and hear rate under different states.

the person is 13 years old [36]. Therefore, the iris diameter can be considered as a constant and thus be used as a reference in a frame of recorded videos [36]. As a consequence, the relative pupil size is invariant to the distance and the angle where the video is recorded.

To illustrate how pupillary response correlates with heart rate, 50 volunteers (27 males and 23 females, aged from 20 to 47) are recruited to measure their pupil size changes and ECG signals in different states, i.e., at rest, during exercise, and after stimulation. As shown in Fig. 2, the average relative pupil size increases with the acceleration of heart rate. This indicates that there is indeed a connection between pupil size and heart rate. Therefore, it is theoretically feasible to infer whether HRV is normal or not based on pupil size series.

In the following section, we elaborate on building a pupil-HRV model based on the deep-learning method.

IV. System Design

In this section, we present the details of PupilHeart's designing. We start with an overview of PupilHeart in Section IV-A. Then, by introducing the data collection in Section IV-B, PupilHeart preprocesses the collected data in Section IV-C. On that basis, a 1-D CNN is customized in Section IV-D to extract pupil series features relevant to HRV. Based on the extracted features, PupilHeart deploys an RNN to build a pupil-HRV model in Section IV-E.

A. Design Overview

The system overview of PupilHeart is illustrated in Fig. 3. PupilHeart consists of four modules: 1) *Data Collection*; 2) *Data Preprocessing*; 3) *Feature Extraction*; and 4) *Pupil-HRV Model*. In *Data Collection*, PupilHeart utilizes collected frames containing user pupils when unlocking phones to obtain relative pupil size series. Then, the collected series are preprocessed in *Data Preprocessing* module by missing values handling, outliers removing, linear interpolation, butterworth lowpass filtering, and labeling. Building on this, in *Feature Extraction*, a 1-D CNN is customized to extract HRV-relating high-dimensional features of pupillary response. As the extracted features are time-related due to the convolutional operation in 1-D CNN, in *Pupil-HRV Model*, an RNN is adopted to model the relation model of pupillary response and HRV.
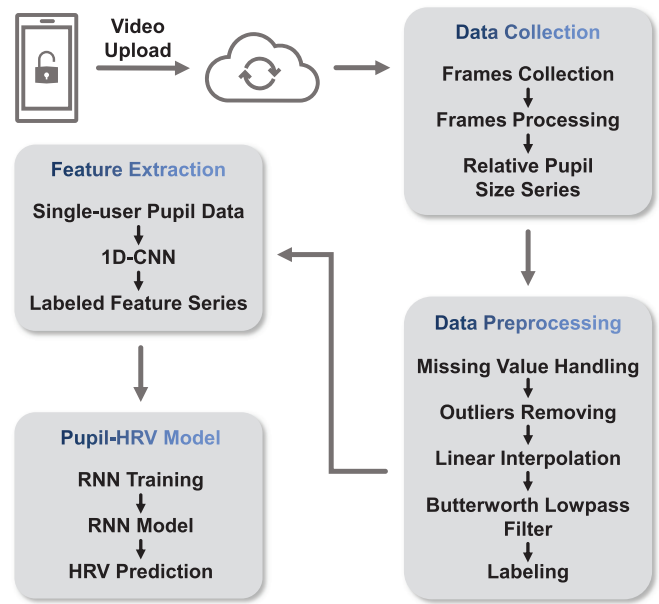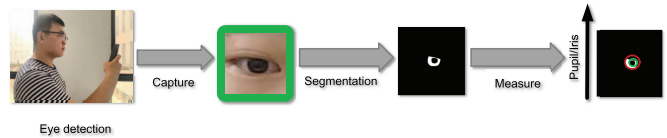

Fig. 3. System architecture of PupilHeart.

Fig. 4. General process of relative pupil size data collection.

B. Data Collection

Fig. 4 shows the general process of relative pupil size data collection. When people unlocking the phone using face identification, PupilHeart captures relative pupil size series by the unlocking face frames and OpenCV's Haar Cassade classifier [37]. Noting that the captured frames contain pupil profiles, a deep learning method—U-net [38], [39] is utilized to segment the pupil and iris. In particular, U-net trains a deep learning network and the generated model effectively convert the eye region into a binary image. Then, the relative pupil size is obtained by an algorithm fitting circles around the iris and pupil. Specifically, the algorithm searches the circle with the smallest area of iris and pupil, which encloses a 2-D point set.

C. Data Preprocessing

After capturing the relative pupil size series, PupilHeart further performs data preprocessing, consisting of missing value handling, outliers removing, linear interpolation, butterworth lowpass filtering, and labeling of relative pupil size series.

1) Missing Value Handling: Since some pupil size data are missing due to blinking and front-facing camera deflection, we consider the amount of missing data for initial filtering. Specifically, if the missing value of the pupil size series exceeds 30%, the data is discarded, otherwise, the data is filled with the mean when the distribution is symmetric, and the data is filled with the median when the distribution is skewed. Note that the discarding of limited missing values has little effect on the validity of data.

2) Outliers Removing: After the initial data filtering, we find that there are still some outliers in data. Therefore, we consider two methods to remove these outliers. We first process the pupil sequence from a coarse-grained perspective. Specifically, the Pauta criterion [40] is utilized, assuming that the measured relative pupil size series as $x_1, x_2, \ldots, x_n$, the arithmetic mean of the series is μ, and the residual error is $v_i = x_i - \mu (i = 1, 2, \ldots, n)$. Then, the standard deviation σ is calculated by Bessel's formula. If the residual error $v_b (1 \le b \le n)$ of a certain measurement x_b satisfies (1), then x_b is considered to be a bad value containing a coarse error and should be discarded

$$|v_b| = |x_b - \mu| > 3\sigma. \tag{1}$$

As for fine-grained outliers removing, we consider the pupil dilation speed outside the median absolute deviation (MAD) as outliers and then discard them [41]. Since blinking is characterized by intersample variation in pupil size, blink filtering can also be achieved by removing samples based on deviations in pupil dilation speed. MAD is defined as (2) shows, where x_i is the ith data of relative pupil size series x. Moreover, the pupil dilation speed is determined as shown in (3) [41], where $d[i]$ is the pupil size at timestamp $t[i]$, and the pupil dilation speed $d'[i]$ is the maximum normalized absolute value compared to the previous or the next sample

$$\text{MAD} = \text{median}(|x_i - \text{median}(x)|) \tag{2}$$

$$d'[i] = \max\left(\left|\frac{d[i] - d[i-1]}{t[i] - t[i-1]}\right|, \left|\frac{d[i+1] - d[i]}{t[i+1] - t[i]}\right|\right). \tag{3}$$

3) Linear Interpolation: After completing the above processing, the relative pupil size series consists of unequally spaced data points in which the data have been removed by the aforementioned processes. To improve the temporal resolution and smoothness of the data, we resample the data points to the original sampling rate (30 Hz) by linear interpolation [42], [43].

4) Butterworth Lowpass Filtering: Since the frequency of pupil size change is at low frequencies, we used a zero-phase butterworth low-pass filter with a cutoff frequency of 4 Hz [44], [45] to filter out high-frequency noise.

5) Labeling: While acquiring the relative pupil size series, the ECG signals are measured using the Scorpio low-power ECG heart rate detection sensor (sampling rate: 1024 Hz) [46]. The two kinds of data are synchronized by transferring them to the master controller (i.e., a laptop) via serial interfaces. That is, when the volunteer unlocks the phone, the phone transmits the recorded pupil data containing the recorded timestamp information to the controller via the interface, while the Scorpio sensor keeps recording the data (also containing the recorded timestamp information) during the experiment. Finally, the ECG data is obtained and synchronized with the pupil data by comparing the timestamp information. The error range of this synchronization method is within 0.03 s. Then, the Pan–Tompkins detection algorithm is utilized to obtain the position of the R waves in ECG signal and thus HRV index SDRR (standard deviation of RR intervals) is calculated [47], [48]. Specifically, the Pan–Tompkins algorithm is a dual-threshold QRS wave detection algorithm with adaptive
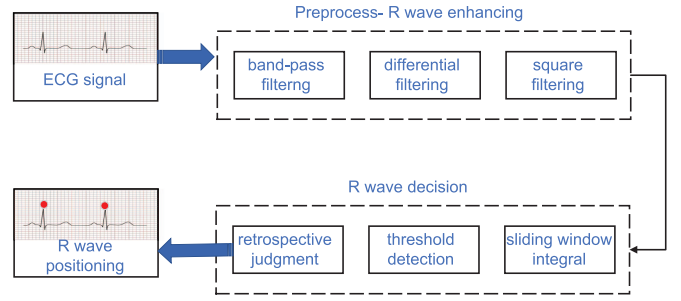
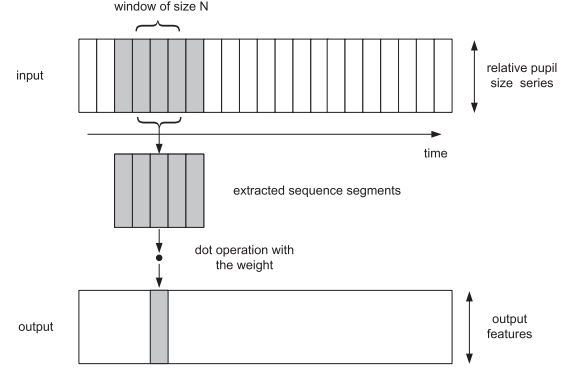

Fig. 5. Pan–Tompkins detection algorithm.

Fig. 6. One layer of 1-D CNN.

property that can be used for R waves processed in real time. The detection algorithm is mainly based on the morphological characteristics of R-waves, including amplitude, slope, and time information. In addition, the algorithm mainly includes two parts: 1) preprocessing to achieve R-wave enhancement and 2) R-wave synthesis decision, and the algorithm flow chart is shown in Fig. 5. After getting the SDRR index of HRV, we judge whether it is within the range of (14 139) ms [3], [49]. If it is within this range, the volunteer's heartbeat is considered to be in a normal state at this time, otherwise it is considered to be in an abnormal state [50], [51].

D. Feature Extraction

Although the coarse relationship between pupil and heartbeat is mentioned in Section III, it is difficult to determine HRV directly by the size of the pupil. Therefore, we consider using a feature extraction method to find out the pupil series features associated with HRV.

A 1-D CNN can be used to extract features of time series [52], [53]. As shown in Fig. 6, a layer of 1-D CNN extracts local 1-D sequence segments, namely, subsequences, from the relative pupil size series according to a window of a certain size, and then performs a dot product with a weight. The output is a segment on the new sequence. After the window is continuously sliding, the feature vector is finally obtained. 1-D CNN is good at recognizing simple patterns in the data and then using them to generate more complex patterns in higher layers. Therefore, 1-D CNN can well perform feature extraction.

The customized 1-D CNN network architecture for feature extraction is shown in Table I. We use the popular rectified

<div style="column: left">

TABLE I
CNN LAYERS AND PARAMETER AMOUNTS

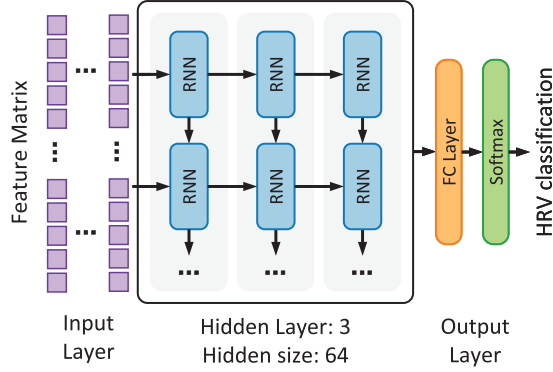| Layer	Layer Type	Output Shape	#Param
1	Conv1D+ReLu	(16, 240)	96
2	Max Pooling	(16, 120)	
3	Dropout	(16, 120)	
4	Batch Normalization	(16, 120)	32
5	Conv1D + ReLU	(32, 120)	2592
6	Max Pooling	(32, 60)	
7	Batch Normalization	(32, 60)	64
8	Flatten	(1920)	
9	Dense + ReLU	(128)	245888
10	Batch Normalization	(128)	256
11	Dense + Softmax	(2)	258

Fig. 7.   RNN containing three hidden layers.

linear unit ReLU as the activation function after each layer of convolution. To save computational cost by reducing the number of parameters for training and inference to lightly deploy the model on mobile devices, we pass the output of each activation function layer through a maximum pooling layer of size 2 for downsampling. Then, after the maximum pooling layer of the first convolutional layer, we add a Dropout layer to prevent overfitting of the neural network. In addition, we also add a batch normalization process to increase the stability of the neural network and speed up the training, which is achieved by subtracting the batch mean and dividing it by the batch standard deviation. At the end of the fully connected layer of the neural network, we use the Softmax activation function to output the classification probabilities for each class. 1-D CNN is trained on a data set containing samples from two classes, namely, the relative pupil size series corresponding to normal and abnormal HRV. To use the model as a general feature extractor, we extract the reciprocal of the trained model as the output value of the second layer, namely, a 1-D feature vector of length 128. The trained model has 249 184 parameters and a size of 1.9 MB, which is portable enough for real-time inference on mobile devices.

E. Pupil-HRV Model

Since the high-dimensional features extracted by 1-D CNN in Section IV-D are time related, and RNN are good at processing time series [54], we use an RNN containing three hidden layers to model pupil size with HRV, as shown in Fig. 7. Specifically, suppose there is small batch of input data $\mathbf{X}_t \in \mathbb{R}^{n \times d}$ at time step t, where n is the number of samples and d is the number of inputs in each sample. Meanwhile,

</div>

<div style="column: right">

the hidden state of the lth hidden layer ($l = 1, 2, 3$) is set to $\mathbf{H}_t^{(l)} \in \mathbb{R}^{n \times h}$, where h is the number of hidden units, and the output layer variable is set to $\mathbf{O}_t \in \mathbb{R}^{n \times q}$, where q is the number of outputs. By setting $\mathbf{H}_t^{(0)} = \mathbf{X}_t$ and the hidden state of the lth hidden layer using the activation function ϕ_l, then

$$\mathbf{H}_t^{(l)} = \phi_l\Big(\mathbf{H}_t^{(l-1)}\mathbf{W}_{xh}^{(l)} + \mathbf{H}_{t-1}^{(l)}\mathbf{W}_{hh}^{(l)} + \mathbf{b}_h^{(l)}\Big) \quad (4)$$

where the weights $\mathbf{W}_{xh}^{(l)} \in \mathbb{R}^{h \times h}$, $\mathbf{W}_{hh}^{(l)} \in \mathbb{R}^{h \times h}$, and the bias $\mathbf{b}_h^{(l)} \in \mathbb{R}^{1 \times h}$ are the model parameters of the lth hidden layer. Finally, the output layer is computed based only on the final hidden state of the lth hidden layer

$$\mathbf{O}_t = \mathbf{H}_t^{(3)}\mathbf{W}_{hq} + \mathbf{b}_q \quad (5)$$

where the weights $\mathbf{W}_{hq} \in \mathbb{R}^{h \times q}$ and the bias $\mathbf{b}_q \in \mathbb{R}^{1 \times q}$ are both model parameters of the output layer.

By completing the pupil-HRV modeling, PupilHeart runs as a daemon. When a user unlock his/her phone adopting PupilHeart to monitoring user's HRV, PupilHeart captures relative pupil size sequences corresponding to each time the user unlock through the front-facing camera. Then by data preprocessing and feature extraction, PupilHeart extracts the high-dimensional features of each pupil size sequence. Upon inputting these features into the RNN mentioned above, it outputs the classification of HRV. Therefore, PupilHeart infers the user's HRV at the time when he/she unlocks phone.

V. EVALUATION

We have prototyped the implementation of PupilHeart on HUAWEI P50. As a proof-of-concept system, the data analysis is performed on a desktop with an Intel i7-5700 CPU and 16 G RAM running Windows 10 with JetBrains PyCharm 2021 software. PupilHeart captures images of users' pupils using the front-facing camera when they unlocking the phone by facial recognition. We first present the experimental setup and evaluation metrics in Section V-A. Then, we perform extensive experiments to estimate the overall performance of PupilHeart, including the accuracy of PupilHeart, and investigate the influence of different factors on performance in Section V-B.

A. Experiment Setup and Metrics

1) Experimental Setting: A total of 60 volunteers (34 females and 26 males) have participated in the evaluation. Moreover, the distribution of volunteers is shown in Table II, from which it can be seen that we recruit volunteers in the age group of 18 to 73 years (including young and middle-aged people) and in different health states to participate in the experiment. The participants have normal vision or wear glasses without color. Participants were compensated based on their participation time in the study ($5 for 2 h) and compliance rate ($0.5 for each completed task). All collected data were kept anonymous and the Institutional Review Board of our university authorized all the study procedures.

The experiments are conducted in a normal quiet office environment. Participants are unlocking the phone under different situations. The overall brightness of ambient and screen light
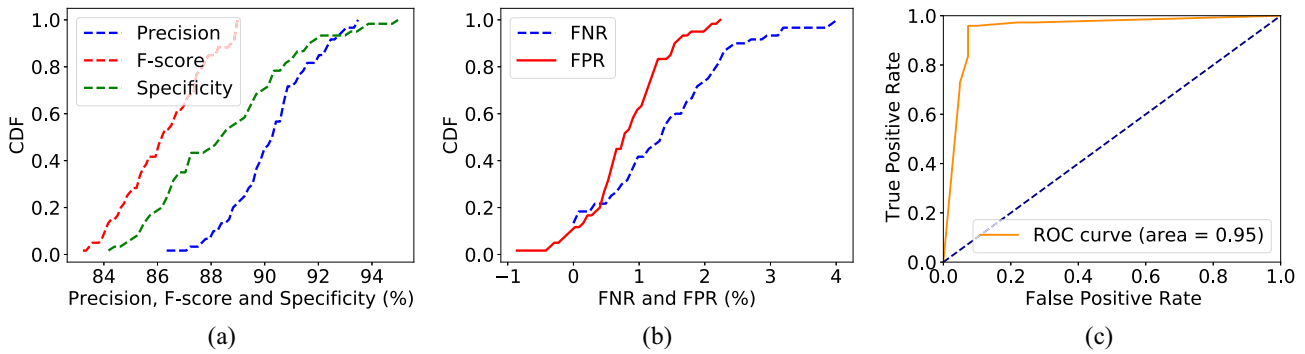
</div>

Fig. 8.   Overall performance of PupilHeart. (a) CDF plot of precision, F-score, and specificity. (b) CDF plot of FNR and FPR. (c) ROC curve.

TABLE II
DEMOGRAPHICS OF VOLUNTEERS IN THE EXPERIMENT

Gender	No.	Age range	No.	Health status	No.
Female	34	18-31	19	Healthy heart	39
Male	26	32-45	13	Unhealthy heart	21
		46-59	17		
		60-73	11		

TABLE III
RESULTS OF PREDICTION ACCURACY

	Mean	Median	Standard Deviation
Precision (%)	90.12	90.26	1.48
F-score (%)	85.93	86.17	1.57
Specificity (%)	88.42	88.35	2.75
FNR (%)	1.37	1.32	1.17
FPR (%)	0.83	0.76	0.61

to participants' eyes is about 240 lux. The distance between participants' eyes and the front facing camera on mobile phone is about 32 cm. Participants are required to unlock the phone when they are at rest, after stimulation, and during exercise. Meanwhile, the front facing camera captures eye area of participants, and the ECG signals (ground truth data) are recorded by the ECG sensor. Specifically, the videos recorded by the camera have a resolution of 720 p and a frame rate of 30 fps. In addition, we use ten times 10-fold cross-validation. The data set is divided into ten mutually exclusive subsets, and one of the subsets is taken for testing, and the other nine subsets are trained, and then the average of the obtained metrics are used as the final evaluation.

2) Evaluation Metrics: PupilHeart adopts RNN to model the relationship between pupil size and HRV. Moreover, as RNN is utilized to classify time series, we evaluate the performance of PupilHeart using typical metrics of binary classifications. In addition, the four parameters of the metrics are true positive (TP), true negative (TN), false positive (FP), and false negative (FN) and are defined as follows (samples with normal HRV are defined as positive classes).

1) *TP:* Samples with normal HRV are correctly classified as positive class.
2) *TN:* Samples with abnormal HRV are correctly classified as negative class.
3) *FP:* Samples with abnormal HRV are incorrectly classified as positive class.
4) *FP:* Samples with normal HRV are incorrectly classified as negative class.

Specifically, the metrics are precision, recall, F-score, specificity, FN rate (FNR), FP rate (FPR), and receiver operating characteristic (ROC) curve. Precision is defined as $P = [(TP)/(TP + FP)]$, describing the ratio of samples with a normal HRV that are predicted correctly. Recall is defined as $R = [(TP)/(TP + FN)]$, manifesting the proportion of normal HRV samples that are correctly predicted. F-score is defined

as $F - \text{score} = [(2P \cdot R)/(P + R)]$, which is a harmonic mean based on the precision and recall. Specificity is defined as specificity $= [(TN)/(FP + TN)]$, which represents the proportion of abnormal HRV samples that are correctly identified, measuring the recognition ability of PupilHeart for abnormal HRV. FPR is defined as $FPR = [(FP)/(TN + FP)]$, describing the proportion of abnormal HRV samples that are predicted as normal. FNR is defined as $FNR = [(FN)/(FN + TP)]$, which describes the rate of normal HRV samples that are incorrectly predicted as abnormal samples. ROC curve is a curve with FPR and TP rate (TPR) as its axes. As a supplementary note, TPR is defined as $TPR = [(TP)/(TP + FN)]$, which is the same as recall. The area under the ROC curve is called AUC, and the larger the AUC, the better the performance of the system.

B. System Performance

We first evaluate the overall performance of PupilHeart in different user states, and then investigate impacts of different factors on the performance.

1) Prediction Accuracy: To estimate the accuracy of PupilHeart's prediction, 60 volunteers are recruited to participate in the experiment. Each volunteer are asked to unlock their phones using the facial recognition in three different states (at rest, after stimulation, and during exercise). Each person unlocks the phone ten times in each state, therefore, there are 1800 pieces of data in total. Morover, ten times 10-fold cross-validation is utilized to calculate the evaluation metrics. The precision, F-score, specificity, FNR, and FPR are calculated. The results are shown in Table III and Fig. 8. The mean values of precision, F-score, specificity, FNR and FPR are 0.9012, 0.8593, 0.8842, 0.0137, and 0.0083, respectively. Moreover, precision, specificity, F-score, FNR and FPR have median values of 0.9026, 0.8617, 0.8835, 0.0132 and 0.0076, respectively. The AUC of the ROC curve is 0.95. These results
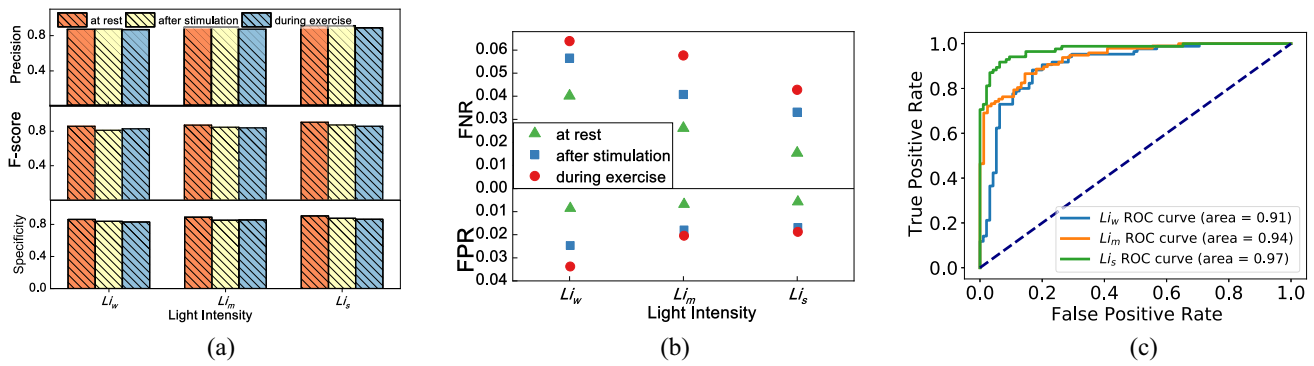
Fig. 9. PupilHeart's performance under different lighting conditions. (a) Precision, F-score, and Specificity. (b) FNR and FPR. (c) ROC curves.
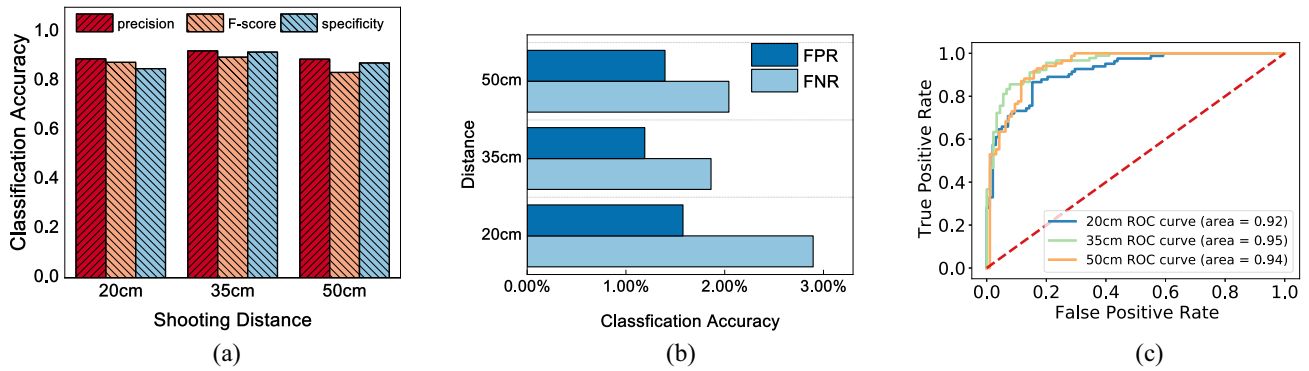

Fig. 10. PupilHeart's performance under different shooting distances. (a) Precision and F-score. (b) FNR and FPR. (c) ROC curves.

illustrate that PupilHeart predicts users' HRVs with a relatively high accuracy after training.

2) Impact of Light Intensity: To investigate the effect of light intensity on the performance of PupilHeart, we set three different light intensities by tuning the brightness of the ambient light. Specifically, we change the light intensity by adjusting the number of lamps in the office, i.e., weak light intensity Li_w (110–150 lux) of one lamp, medium light intensity Li_m (220–260 lux) of two lamps, strong light intensity Li_s (280–300 lux) of three lamps. 60 volunteers aged from 18 to 73 participate in the experiment. Each volunteer unlocks their phone under these three different lighting conditions for ten times. The precision, F-score, specificity, FNR and FPR are measured, and the results are shown in Fig. 9. As presented in Fig. 9, the lighting conditions do have an impact on the performance of PupilHeart. As the illumination intensifies, the precision, F-score, and specificity are rising under different states, while the FPR and FNR are decreasing, demonstrating that under certain illumination conditions, the stronger the illumination is, the better the performance of PupilHeart. Meanwhile, the AUCs of these three light conditions are also increasing with the light intensities. This is due to the fact that PupilHeart can detect the face more clearly when the light is strong, and thus can obtain more accurate relative pupil size values. In addition, we find that the performance of PupilHeart remains relatively stable under different user states.

3) Impact of Shooting Distance: The general face unlocking distance for mobile phones is 20–50 cm [55], and the distance from the front-facing camera affects the clarity of

the captured image and thus the accuracy of the obtained pupil size data. Therefore, in this section, we discuss the performance of PupilHeart at three different distances (20, 35, and 50 cm). A total of 60 volunteers between the ages of 18 and 73 participate in the experiment. Each volunteer unlock the phone using facial recognition for ten times at three different distances (each volunteer is not necessarily in the same state) and the light intensity is kept at a medium level Li_m by allowing two lamps on in the office, so there are 1800 pieces of data in total.

The results of the experiment are shown in Fig. 10. From the figure, it can be observed that PupilHeart's performance reaches it highest level at 35 cm. When the user is 20 or 50 cm away from the front-facing camera, PupilHeart's performance is slightly disrupted. This is because too long or too short a shooting distance can affect the imaging of the camera and thus the accuracy of the captured pupil size sequence, and therefore the performance of PupilHeart.

VI. DISCUSSIONS

In this section, we discuss the effects of various environment conditions on PupilHeart.

1) *Extreme Light Intensity:* In our experiments, we investigate the performance of PupilHeart over a certain range of light intensities (110–300 lux). When the light intensity is at extremely high or low levels, for example, when the user is in the dark or in strong outdoor light, although normal face recognition will not be affected (because face unlock uses an infrared camera that can unlock the phone in the dark or in bright light), but

the image of users' pupils collected by PupilHeart will be blurred. Therefore, in future work, we will consider using the same infrared camera for capturing pupil data as for face recognition.

2) *Extreme Shooting Distance:* We consider the performance of PupilHeart when user normally uses facial recognition to unlock phones. However, when user is very close to the phone screen, PupilHeart will not be able to detect the user's face and therefore the pupils, and the phone's facial recognition function will not work as well. Furthermore, when the user is far from the phone, PupilHeart captures blurred face images due to the limited resolution of the front camera, and the facial recognition is also not available in this case. Therefore, PupilHeart works fine under normal use of facial unlock.

3) *User Wearing Glasses:* Participants in the experiment wear regular glasses or no glasses. In real life, however, the resolution of the eyes in the captured images is reduced when the user wears tinted glasses such as sunglasses. The current facial recognition technology already supports most sunglasses by utilizing infrared cameras and thus we will take this situation into account in future work.

4) *Camera Resolution and Frame Rate:* Since PupilHeart is running during face unlock, and the camera we use is the front-facing camera of the phone instead of the infrared camera used for face unlock, which has different specifications, we discuss the effect of different resolutions and frame rates of the camera. First, we record videos with different front-facing cameras resolutions of 360P, 480P, 720P, and 1080P at a fixed frame rate of 30 fps. The results show that the videos recorded by the 360P and 480P cameras are too blurry, and thus PupilHeart can not segment the user's pupils and irises well. In addition, to explore the effect of different frame rates on PupilHeart, we record videos at 30, 60, and 120 fps using the front camera of the phone with a fixed resolution of 720P, The results showed limited difference. However, we plan to investigate these issues and mobile phone diversity in a more in-depth evaluation in future work.

5) *Limitation of HRV-Based Method:* Although PupilHeart can be a relatively accurate measure of whether HRV is within the normal range, there are some shortcomings in the HRV-based approach. In general, abnormal HRV does not lead to a medical emergency, but it can be a sign of current health problems or future problems. For instance, low HRV is considered a sign of current or future health problems because it shows your body is less resilient and struggles to handle changing situations. It is also more common in people who have higher resting heart rates. That is because when your heart is beating faster, there is less time between beats, reducing the opportunity for variability. This is often the case with conditions like diabetes, high blood pressure, heart arrhythmia, asthma, anxiety, and depression. It is also important to remember that most consumer-grade devices that track HRV are not as sensitive as an electrocardiogram (EKG). It is important to keep in mind that heart rhythm is very complex. While we can find devices and apps that track HRV, healthcare providers are best qualified to watch our heart rate and make recommendations on what we can and should do about it.

VII. Conclusion

In this article, we have proposed PupilHeart as a computer-vision-based mobile HRV monitoring system, including a mobile terminal and a server side. On the mobile terminal, during face recognition, PupilHeart has collected pupil size information through the front facing camera on mobile phones. On the server side, after preprocessing the raw pupil size data, PupilHeart has extracted high-dimension features using 1-D CNN, and based on this, has built a pupil-HRV model by RNN. On that basis, PupilHeart has achieved daily HRV monitoring. We have prototyped PupilHeart and conducted experimental and field studies to thoroughly evaluate the efficacy of it by recruiting 60 volunteers. The overall results have shown that PupilHeart can accurately predict a user's HRV when unlocking phones using face recognition. In general, PupilHeart provides us with a prototype for exploring pupil size and HRV, shedding lights on a viable yet innovative idea for realizing mobile HRV monitoring systems. In future works, we will expand the diversity of experiments in terms of devices, subjects, and environment conditions to further improve our PupilHeart system.

References

[1] J. I. Hoffman and S. Kaplan, "The incidence of congenital heart disease," *J. Amer. College Cardiol.*, vol. 39, no. 12, pp. 1890–1900, 2002.

[2] *WHO Methods and Data Sources for Global Burden of Disease Estimates 2000–2011*, Dept. Health Statist. Inf. Syst., WHO, Geneva, Switzerland, 2013.

[3] R. Castaldo, P. Melillo, U. Bracale, M. Caserta, M. Triassi, and L. Pecchia, "Acute mental stress assessment via short term HRV analysis in healthy adults: A systematic review with meta-analysis," *Biomed. Signal Process. Control*, vol. 18, pp. 370–377, Apr. 2015.

[4] F. Wang, X. Zeng, C. Wu, B. Wang, and K. R. Liu, "mmHRV: Contactless heart rate variability monitoring using millimeter-wave radio," *IEEE Internet Things J.*, vol. 8, no. 22, pp. 16623–16636, Nov. 2021.

[5] F. Lombardi, "Clinical implications of present physiological understanding of HRV components," *Cardiac Electrophysiol. Rev.*, vol. 6, no. 3, pp. 245–249, 2002.

[6] E. Kristal-Boneh, M. Raifel, P. Froom, and J. Ribak, "Heart rate variability in health and disease," *Scand. J. Work Environ. Health*, vol. 21, no. 2, pp. 85–95, 1995.

[7] M. P. Tarvainen, P. O. Ranta-Aho, and P. A. Karjalainen, "An advanced detrending method with application to HRV analysis," *IEEE Trans. Biomed. Eng.*, vol. 49, no. 2, pp. 172–175, Feb. 2002.

[8] B. Makivić, M. Nikić Djordjević, and M. S. Willis, "Heart rate variability (HRV) as a tool for diagnostic and monitoring performance in sport and physical activities," *J. Exercise Physiol. Online*, vol. 16, no. 3, p. 103, 2013.

[9] P. J. Zimetbaum and M. E. Josephson, "Use of the electrocardiogram in acute myocardial infarction," *New England J. Med.*, vol. 348, no. 10, pp. 933–940, 2003.

[10] E. Çiçekli and E. Emre, "The effect of tension variability for sleep quality in headache patients: A Holter monitoring study," *Medicine*, vol. 101, no. 30, 2022, Art. no. e29876.

[11] Y. K. Peker, G. Bello, and A. J. Perez, "On the security of Bluetooth low energy in two consumer wearable heart rate monitors/sensing devices," *Sensors*, vol. 22, no. 3, p. 988, 2022.

[12] Y. Gao et al., "Heart monitor using flexible capacitive ECG electrodes," *IEEE Trans. Instrum. Meas.*, vol. 69, no. 7, pp. 4314–4323, Jul. 2020.

[13] J. Parak, A. Tarniceriu, P. Renevey, M. Bertschi, R. Delgado-Gonzalo, and I. Korhonen, "Evaluation of the beat-to-beat detection accuracy of PulseOn wearable optical heart rate monitor," in *Proc. IEEE 37th Annu. Int. Conf. Eng. Med. Biol. Soc. (EMBC)*, 2015, pp. 8099–8102.

[14] W. Huang, W. Tang, H. Jiang, J. Luo, and Y. Zhang, "Stop deceiving! An effective defense scheme against voice impersonation attacks on smart devices," *IEEE Internet Things J.*, vol. 9, no. 7, pp. 5304–5314, Apr. 2022.

[15] C.-A. Wang, T. Baird, J. Huang, J. D. Coutinho, D. C. Brien, and D. P. Munoz, "Arousal effects on pupil size, heart rate, and skin conductance in an emotional face task," *Front. Neurol.*, vol. 9, p. 1029, Dec. 2018.

[16] W. Huang, W. Tang, K. Zhang, H. Zhu, and Y. Zhang, "Thwarting unauthorized voice eavesdropping via touch sensing in mobile systems," in *Proc. IEEE Conf. Comput. Commun.*, 2022, pp. 31–40.

[17] M. Harbach, A. De Luca, and S. Egelman, "The anatomy of smartphone unlocking: A field study of android lock screens," in *Proc. CHI Conf. Human Factors Comput. Syst.*, 2016, pp. 4806–4817.

[18] "By 2024, How many smartphone owners will use biometrics?" 2020. [Online]. Available: https://www.paymentsjournal.com/by-2024-how-many-smartphone-owners-will-use-biometrics/

[19] L. F. Jimenez, A. Parnandi, and R. Gutierrez-Osuna. "Extracting heartrate and respiration rate using a cell phone camera." 2013. [Online]. Available: http://dreuarchive.cra.org/2013/Jimenez/documents/EXTRACTING%20HEART%20RATE%20AND%20RESPIRATION%20RATE%20USING%20A%20CELL%20PHONE%20CAMERA.pdf

[20] J. B. Bolkhovsky, C. G. Scully, and K. H. Chon, "Statistical analysis of heart rate and heart rate variability monitoring through the use of smart phone cameras," in *Proc. Annu. Int. Conf. IEEE Eng. Med. Biol. Soc.*, 2012, pp. 1610–1613.

[21] D. J. Plews, B. Scott, M. Altini, M. Wood, A. E. Kilding, and P. B. Laursen, "Comparison of heart-rate-variability recording with smartphone photoplethysmography, polar H7 chest strap, and electrocardiography," *Int. J. Sports Physiol. Perform.*, vol. 12, no. 10, pp. 1324–1328, 2017.

[22] A. S. Perrotta, A. T. Jeklin, B. A. Hives, L. E. Meanwell, and D. E. Warburton, "Validity of the elite HRV smartphone application for examining heart rate variability in a field-based setting," *J. Strength Conditioning Res.*, vol. 31, no. 8, pp. 2296–2302, 2017.

[23] F. Guede-Fernández, V. Ferrer-Mileo, J. Ramos-Castro, M. Fernández-Chimeno, and M. A. García-González, "Real time heart rate variability assessment from android smartphone camera photoplethysmography: Postural and device influences," in *Proc. 37th Annu. Int. Conf. IEEE Eng. Med. Biol. Soc. (EMBC)*, 2015, pp. 7332–7335.

[24] L. H. R. Batista, W. J. R. Domingues, A. D. A. C. e Silva, K. A. T. Lopes, M. L. de Castro Amorim, and M. Rossato, "Heart rate variability responses determined by photoplethysmography in people with spinal cord injury," *Biomed. Signal Process. Control*, vol. 69, Jun. 2021, Art. no. 102845.

[25] V. P. Rachim, J.-H. Baek, Y. S. Kim, Y. Kim, and S.-M. Park, "High sampling rate smartphone-PPG via built-in rolling shutter image sensor," *IEEE Internet Things J.*, vol. 10, no. 1, pp. 512–525, Jan. 2023.

[26] J. Ramos-Castro et al., "Heart rate variability analysis using a seismocardiogram signal," in *Proc. Annu. Int. Conf. IEEE Eng. Med. Biol. Soc.*, 2012, pp. 5642–5645.

[27] L. Wang et al., "Unlock with your heart: Heartbeat-based authentication on commercial mobile phones," *Proc. ACM Interactive, Mobile, Wearable Ubiquitous Technol.*, vol. 2, no. 3, pp. 1–22, 2018.

[28] M. Scarpetta, M. Spadavecchia, G. Andria, M. Ragolia, and N. Giaquinto, "Accurate simultaneous measurement of heartbeat and respiratory intervals using a smartphone," *J. Instrum.*, vol. 17, no. 7, 2022, Art. no. P07020.

[29] M. Urzeniczok, S. Sieciński, and P. Kostka, "Heart rate measurement based on embedded accelerometer in a smartphone," in *Proc. Int. Conf. Inf. Technol. Biomed.*, 2022, pp. 443–454.

[30] A. Schumann, S. Kietzer, J. Ebel, and K. J. Bär, "Sympathetic and parasympathetic modulation of pupillary unrest," *Front. Neurosci.*, vol. 14, p. 178, Mar. 2020.

[31] K. Hung and Y.-T. Zhang, "Preliminary investigation of pupil size variability: Toward non-contact assessment of cardiovascular variability," in *Proc. 3rd IEEE/EMBS Int. Summer School Med. Devices Biosensors*, 2006, pp. 137–140.

[32] N. Urrestilla and D. St-Onge, "Measuring cognitive load: Heart-rate variability and pupillometry assessment," in *Proc. Int. Conf. Multimodal Interact. Companion Publ.*, 2020, pp. 405–410.

[33] C. Daluwatte, J. Miles, and G. Yao, "Simultaneously measured pupillary light reflex and heart rate variability in healthy children," *Physiol. Meas.*, vol. 33, no. 6, p. 1043, 2012.

[34] A. Parnandi and R. Gutierrez-Osuna, "Contactless measurement of heart rate variability from pupillary fluctuations," in *Proc. Humaine Assoc. Conf. Affect. Comput. Intell. Interact.*, 2013, pp. 191–196.

[35] A. R. Mitz, R. V. Chacko, P. T. Putnam, P. H. Rudebeck, and E. A. Murray, "Using pupil size and heart rate to infer affective states during behavioral neurophysiology and neuropsychology experiments," *J. Neurosci. Methods*, vol. 279, pp. 1–12, Mar. 2017.

[36] V. W. S. Tseng, S. Abdullah, J. M. R. Costa, and T. Choudhury, "AlertnessScanner: What do your pupils tell about your alertness," in *Proc. 20th Int. Conf. Human-Comput. Interact. Mobile Devices Services*, 2018, pp. 41:1–41:11.

[37] "Haar cascade classifier." 2017. [Online]. Available: http://docs.opencv.org/2.4/doc/tutorials/objdetect/cascade_classifier/cascade_classifier.html

[38] O. Ronneberger, P. Fischer, and T. Brox, "U-Net: Convolutional networks for biomedical image segmentation," in *Proc. 18th Int. Conf. Med. Image Comput. Comput.-Assisted Intervention (MICCAI)*, Munich, Germany, 2015, pp. 234–241.
O. Ronneberger, P. Fischer, and T. Brox, "U-net: Convolutional networks for biomedical image segmentation," in Medical Image Computing and Computer-Assisted Intervention-MICCAI 2015: 18th International Conference, Munich, Germany, October 5-9, 2015, Proceedings, Part III 18. Springer, 2015, pp. 234-241.

[39] S. Ding, H. Wang, H. Lu, M. Nappi, and S. Wan, "Two path gland segmentation algorithm of colon pathological image based on local semantic guidance," *IEEE J. Biomed. Health Inform.*, vol. 27, no. 4, pp. 1701–1708, Apr. 2023.

[40] C. Shen, X. Bao, J. Tan, S. Liu, and Z. Liu, "Two noise-robust axial scanning multi-image phase retrieval algorithms based on Pauta criterion and smoothness constraint," *Opt. Exp.*, vol. 25, no. 14, pp. 16235–16249, 2017.

[41] M. E. Kret and E. E. Sjak-Shie, "Preprocessing pupil size data: Guidelines and code," *Behav. Res. Methods*, vol. 51, no. 3, pp. 1336–1342, 2019.

[42] T. Blu, P. Thévenaz, and M. Unser, "Linear interpolation revitalized," *IEEE Trans. Image Process.*, vol. 13, pp. 710–719, 2004.

[43] Y. Liu, T. Dillon, W. Yu, W. Rahayu, and F. Mostafa, "Missing value imputation for industrial IoT sensor data with large gaps," *IEEE Internet Things J.*, vol. 7, no. 8, pp. 6855–6867, Aug. 2020.

[44] I. Jackson and S. Sirois, "Infant cognition: Going full factorial with pupil dilation," *Develop. Sci.*, vol. 12, no. 4, pp. 670–679, 2009.

[45] Y. Zhao, J. Xu, J. Wu, J. Hao, and H. Qian, "Enhancing camera-based multimodal indoor localization with device-free movement measurement using WiFi," *IEEE Internet Things J.*, vol. 7, no. 2, pp. 1024–1038, Feb. 2020.

[46] "Scorpio low-power ECG heart rate detection sensor." 2022. [Online]. Available: https://www.sichiray.com/6.

[47] H. Sedghamiz. "MATLAB implementation of pan tompkins ECG QRS detector." 2014. [Online]. Available: https://frmathworks.com/matlabcentral/fileexchange/45840-complete-pan-tompkins-implementationecg-qrs-detector

[48] W. Ning, S. Li, D. Wei, L. Z. Guo, and H. Chen, "Automatic detection of congestive heart failure based on a hybrid deep learning algorithm in the Internet of Medical Things," *IEEE Internet Things J.*, vol. 8, no. 16, pp. 12550–12558, Aug. 2021.

[49] M. S. Mahmud, H. Wang, A. Esfar-E-Alam, and H. Fang, "A wireless health monitoring system using mobile phone accessories," *IEEE Internet Things J.*, vol. 4, no. 6, pp. 2009–2018, Dec. 2017.

[50] C. Wu, Z. Yuan, S. Wan, L. Wang, and W. Zhang, "Anti-jamming heart rate estimation using a spatial–temporal fusion network," *Comput. Vis. Image Understand.*, vol. 216, Feb. 2022, Art. no. 103327.

[51] W. Huang, Y. Zhang, and S. Wan, "A sorting fuzzy min-max model in an embedded system for atrial fibrillation detection," *ACM Trans. Multimedia Comput., Commun., Appl.*, vol. 18, no. 2S, pp. 1–18, 2022.

[52] B. Zhou, J. Lohokare, R. Gao, and F. Ye, "Echoprint: Two-factor authentication using acoustics and vision on smartphones," in *Proc. 24th Annu. Int. Conf. Mobile Comput. Netw.*, 2018, pp. 321–336.

[53] J. Zhu, X. Lou, and W. Ye, "Lightweight deep learning model in mobile-edge computing for radar-based human activity recognition," *IEEE Internet Things J.*, vol. 8, no. 15, pp. 12350–12359, Aug. 2021.

[54] A. A. Cook, G. Mısırlı, and Z. Fan, "Anomaly detection for IoT time-series data: A survey," *IEEE Internet Things J.*, vol. 7, no. 7, pp. 6481–6494, Jul. 2020.

[55] R. D. Findling and R. Mayrhofer, "Towards pan shot face unlock: Using biometric face information from different perspectives to unlock mobile devices," *Int. J. Pervasive Comput. Commun.*, vol. 9, no. 3, pp. 190–208, 2013.

Xiangyu Shen is currently pursuing the Ph.D. degree in computer science and technology with the College of Computer Science and Electronic Engineer, Hunan University, Changsha, China.

He has published papers in IEEE TVT 2018 and IEEE ICDCS 2021. His research interests focus on mobile sensing, mobile computing, and machine learning.

Hongbo Jiang (Senior Member, IEEE) received the Ph.D. degree from Case Western Reserve University, Cleveland, OH, USA, in 2008.

He is currently a Full Professor with the College of Computer Science and Electronic Engineering, Hunan University, Changsha, China. He was a Professor with the Huazhong University of Science and Technology, Wuhan, China. His current research focuses on computer networking, especially, wireless networks, data science in Internet of Things, and mobile computing.

Prof. Jiang has been serving on the editorial board of IEEE/ACM Transactions on Networking, IEEE Transactions on Mobile Computing, *ACM Transactions on Sensor Networks*, IEEE Transactions on Network Science and Engineering, IEEE Transactions on Intelligent Transportation Systems, and IEEE Internet of Things Journal. He was also invited to serve on the TPC of IEEE INFOCOM, ACM WWW, ACM/IEEE MobiHoc, IEEE ICDCS, and IEEE ICNP. He is an Elected Fellow of The Institution of Engineering and Technology, the Fellow of The British Computer Society, the Senior Member of ACM, and a Full Member of IFIP TC6 WG6.2.

Daibo Liu (Member, IEEE) received the Ph.D. degree in computer science and engineering from the University of Electronic Science and Technology of China, Chengdu, China, in 2018.

He was a Visiting Researcher with the School of Software, Tsinghua University, Beijing, China, from 2014 to 2016, and the Department of Electrical and Computer Engineering, University of Wisconsin-Madison, Madison, WI, USA, from 2016 to 2017. He is currently an Assistant Professor with the College of Computer Science and Electronic Engineering, Hunan University, Changsha, China. His research interests cover the broad areas of low power wireless networks, mobile and pervasive computing, and system security.

Dr. Liu is a member of the ACM.

Kehua Yang received the Ph.D. degree in computer science and engineering from Southeast University, Nanjing, China, in 2005.

He is currently an Associate Professor with the College of Computer Science and Electronic Engineering, Hunan University, Changsha, China. His major research interests includes embedded systems, cyber–physical systems, and automotive systems.

Feiyang Deng received the B.S. degree in electromagnetic field and wireless technology from Harbin Institute of Technology, Harbin, China, in 2019. He is currently pursuing the Ph.D. degree with the City University of Hong Kong, Hong Kong.

His research interests include antenna, millimeter-wave radar, machine learning, and computer vision.
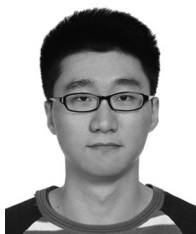
Taiyuan Zhang received the B.S. degree from Hubei University, Wuhan, China, in 2020. He is currently pursuing the M.S. degree with the College of Computer Science and Electronic Engineering, Hunan University, Changsha, China.

His research interests include mobile and wireless networks, especially smart sensing in mobile systems.

Zhu Xiao (Senior Member, IEEE) received the M.S. and Ph.D. degrees in communication and information systems from Xidian University, Xi'an, China, in 2007 and 2009, respectively.

From 2010 to 2012, he was a Research Fellow with the Department of Computer Science and Technology, University of Bedfordshire, Luton, U.K. He is currently an Associate Professor with the College of Computer Science and Electronic Engineering, Hunan University, Changsha, China. His research interests include mobile communications, wireless localization, Internet of Vehicles, and mobile computing.
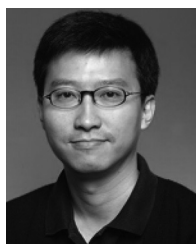
John C. S. Lui (Fellow, IEEE) was born in Hong Kong. He received the Ph.D. degree in computer science from the University of California, Los Angeles, CA, USA, in 1992.

He is currently the Choh-Ming Li Professor with the Department of Computer Science and Engineering, The Chinese University of Hong Kong (CUHK), Hong Kong. He was the Chairman of the Department from 2005 to 2011. His current research interests are in communication networks, network/system security (e.g., cloud security, mobile security, etc.), network economics, network sciences (e.g., online social networks, information spreading, etc.), cloud computing, large-scale distributed systems, and performance evaluation theory.

Prof. Lui received various departmental teaching awards and the CUHK Vice-Chancellors Exemplary Teaching Award. He is also a co-recipient of the Best Paper Award in the IFIP WG 7.3 Performance 2005, IEEE/IFIP NOMS 2006, and SIMPLEX 2013. He is an elected member of the IFIP WG 7.3, a Fellow of the Association for Computing Machinery (ACM), a Senior Research Fellow of the Croucher Foundation, and was the Chair of the ACM SIGMETRICS. He has been serving in the Editorial Board of the IEEE/ACM Transactions on Networking, IEEE Transactions on Computers, IEEE Transactions on Parallel and Distributed Systems, *Performance Evaluation*, and the *International Journal of Network Security*.

Jiangchuan Liu (Fellow, IEEE) received the B.Eng. degree (cum laude) in computer science from Tsinghua University, Beijing, China, in 1999, and the Ph.D. degree in computer science from The Hong Kong University of Science and Technology, Hong Kong, in 2003.

He is a University Professor with the School of Computing Science, Simon Fraser University, Burnaby, BC, Canada. He was an EMC-Endowed Visiting Chair Professor with Tsinghua University, Beijing, from 2013 to 2016. In the past, he worked as an Assistant Professor with The Chinese University of Hong Kong, Hong Kong, and as a Research Fellow with Microsoft Research Asia. His research interests include multimedia systems and networks, cloud and edge computing, social networking, online gaming, and Internet of Things/RFID/backscatter.

Dr. Liu is a co-recipient of the inaugural Test of Time Paper Award of IEEE INFOCOM in 2015, ACM SIGMM TOMCCAP Nicolas D. Georganas Best Paper Award in 2013, and the ACM Multimedia Best Paper Award in 2012. He has served on the editorial boards of IEEE/ACM Transactions on Networking, IEEE Transactions on Big Data, IEEE Transactions on Multimedia, IEEE Communications Surveys and Tutorials, and IEEE Internet of Things Journal. He is a Steering Committee Member of IEEE Transactions on Mobile Computing and the Steering Committee Chair of IEEE/ACM IWQoS from 2015 to 2017. He is a TPC Co-Chair of IEEE INFOCOM'2021. He is a Fellow of The Canadian Academy of Engineering and an NSERC E.W.R. Steacie Memorial Fellow.

Schahram Dustdar (Fellow, IEEE) received the Ph.D. degree in business informatics from the University of Linz, Linz, Austria, in 1992.

He is currently a Full Professor of Computer Science (informatics) with a focus on Internet technologies heading the Distributed Systems Group, TU Wien, Wein, Austria. He has been the Chairman of the Informatics Section of the Academia Europaea since December 2016.

Prof. Dustdar was a recipient of the ACM Distinguished Scientist Award in 2009 and the IBM Faculty Award in 2012. He is an Associate Editor of the IEEE TRANSACTIONS ON SERVICES COMPUTING, *ACM Transactions on the Web*, and *ACM Transactions on Internet Technology*. He is on the Editorial Board of IEEE. He has been a member of the IEEE Conference Activities Committee since 2016, the Section Committee of Informatics of the Academia Europaea since 2015, and the Academia Europaea: The Academy of Europe, Informatics Section since 2013.

Jun Luo (Senior Member, IEEE) received the B.S. and M.S. degrees in electrical engineering from Tsinghua University, Beijing, China, in 1997 and 2000, respectively, and the Ph.D. degree in computer science from EPFL (Swiss Federal Institute of Technology in Lausanne), Lausanne, Switzerland, in 2006.

From 2006 to 2008, he has worked as a Postdoctoral Research Fellow with the Department of Electrical and Computer Engineering, University of Waterloo, Waterloo, ON, Canada. In 2008, he joined the faculty of the School of Computer Science and Engineering, Nanyang Technological University, Singapore, where he is currently an Associate Professor. His research interests include mobile and pervasive computing, wireless networking, machine learning and computer vision, as well as applied operations research. More information can be found at http://www.ntu.edu.sg/home/junluo.